POWER ELECTRONICS AND DRIVES
2(37), No. 1, 2017 DOI: 10.5277/PED170112

# FILTERED INTEGRAL SLIDING MODE CONTROL IN A TWO-MASS DRIVE SYSTEM*

PAWEŁ DRÓŻDŻ, KRZYSZTOF SZABAT

Wrocław University of Science and Technology,
Wybrzeże Wyspiańskiego 27, 50-370 Wrocław, Poland,
e-mail addresses: pawel.drozdz@pwr.edu.pl; krzysztof.szabat@pwr.edu.pl

**Abstract:** The paper presents issues related to the application of filtered integral sliding mode control to a two-mass drive system. A classical control structure has been presented and its design procedure is shown in detail. The properties of the classical structure, in which the chattering phenomenon seems to be a big drawback, have been summarized. In order to eliminate this phenomenon, an output low--pass filter has been proposed and the performance of this system has been tested. In order to improve its characteristics, an adaptive low-pass filter has been proposed. The bandwidth of the filter was changed on-line by the fuzzy system according to the current state of the plant. During the steady-states, the bandwidth is low to eliminate chattering effect, and during transients higher in order to ensure the fast dynamics of the plant.

**Keywords:** *filtered integral sliding mode control, integral sliding mode control, two-mass system, chattering alleviation*

## 1. INTRODUCTION

Today's industrial requirements in the field of robustness, reliability and dynamics of machines are still increasing. Thus, it is very important to predict in the project phase any problems that can arise during the operation of the system. Many researchers focus on deploying methods which are robust and dynamic enough [1–10]. In the field of drive systems, lots of projects omit the existence of elasticity of the coupling between the motor and the load. However, there is a wide group of drives in which this approach is unacceptable, i.e., robots, conveyor belts, cranes, and other [11]. Variable parameters of the plant additionally complicate the control problem. Therefore, a control method robust to parameter mismatch should be selected. Specifically, sliding mode control (SMC) is popular in many applications [1–8, 10, 11].

The SMC method was first published in 1953 by Flugge-Lotz [12] and the research was continued by Emelyanov, Utkin, Itkis and several other co-researchers from the

*Manuscript received: May 5, 2017; accepted: July 17, 2017.

Soviet Union [10, 13]. As the studies showed, the SMC ensures insensitivity to parametric variation and external disturbances [1–10, 13]. This quality together with great control dynamics make it a very attractive control method because it meets modern, high requirements. Unfortunately, there is also one shortcoming of such control method, namely – the chatter effect. In practical engineering systems, the chattering may cause damage to system components [10]. However, owing to the qualities of the SMC, many efforts have been made to minimize the chattering, e.g. [1, 2, 9, 14]. In addition, this method is still being developed by many scientists, who have been trying to implement it in many advanced, practical applications working in difficult environments, e.g., an underwater vehicle [3], a re-entry vehicle [4], a steered-by-wire road vehicle [5].

Some papers could also be listed as ones dealing with the SMC application to drives with an elastic coupling: involving a motor drive in an observer-based SMC structure [6], describing the application of the SMC in wind turbine controlling [7], investigating an integral sliding mode controller (ISMC) for a two-mass system [8].

The advanced control structures [8, 15] allowing damping torsional vibrations effectively need information of the state vector of the plant. Various estimation techniques such as the Luenberger observer, Kalman filter, neural networks or fuzzy systems can be used. The proper selection of the estimator depends on the design requirements. Among the above mentioned concepts, the Kalman filter [11] is said to be robust to measurement and parameter noises.

In this paper, ISMC with an adaptive low pass filter (LPF) has been proposed. Incorporating a LPF at output, allows one to significantly alleviate the chattering level in the transient of an electromagnetic torque and suppress torsional torque amplitude, hence, drive exploitation time is lengthened. The bandwidth of the filter is being adapted during the operation in order to keep desired dynamics (in dynamic states) and alleviate the oscillations level (in static states). The adjusting process is continued by a fuzzy system. The Kalman filter was selected as an observer because of its good performance while operating in disturbed conditions [11].

## 2. PROBLEM STATEMENT

### 2.1. MATHEMATICAL MODELS OF THE PLANT AND THE CONTROL STRUCTURE

A plant under consideration is a two-mass drive system with an elastic joint. The model is described in per-unit system, presented in more detail elsewhere [16]. In order to emulate the real conditions during simulations, viscous and the Coulomb frictions were introduced into the model (1).

$$\underbrace{\begin{bmatrix}\dot{\omega}_2\\ \dot{m}_s\\ \dot{\omega}_1\\ \dot{m}_e\end{bmatrix}}_{\dot{\mathbf{x}}} = \underbrace{\begin{bmatrix}0 & 1/T_2 & 0 & 0\\ -1/T_c & 0 & 1/T_c & 0\\ 0 & -1/T_1 & 0 & 1/T_1\\ 0 & 0 & 0 & -1/T_{me}\end{bmatrix}}_{\mathbf{A}} \underbrace{\begin{bmatrix}\omega_2\\ m_s\\ \omega_1\\ m_e\end{bmatrix}}_{\mathbf{x}} + \underbrace{\begin{bmatrix}0\\0\\0\\1/T_{me}\end{bmatrix}}_{\mathbf{B}} \underbrace{m_e^{\text{ref}}}_{u} + \underbrace{\begin{bmatrix}-1/T_2 & 0 & -1/T_2 & 0\\ 0 & 0 & 0 & 0\\ 0 & -1/T_1 & 0 & 0\\ 0 & 0 & 0 & 0\end{bmatrix}}_{\mathbf{D}} \underbrace{\begin{bmatrix}m_L\\ m_{f1}\\ m_{f2}\\ 0\end{bmatrix}}_{\mathbf{z}} \tag{1}$$

where: $\omega_1$, $\omega_2$ – angular velocities of the motor and load, $m_e$, $m_s$, $m_L$ – electromagnetic, shaft and load torques, $m_{f1}$, $m_{f2}$ – friction torques of the motor and load, $T_1$, $T_2$, $T_c$ – mechanical time constants of the motor, load and shaft, $T_{me}$ – time constant of an electromagnetic torque control loop, $m_e^{\text{ref}}$ – reference electromagnetic torque, **x** – state vector, **A** – state matrix, **B** – input matrix, **D** – disturbance matrix, **z** – disturbance vector.

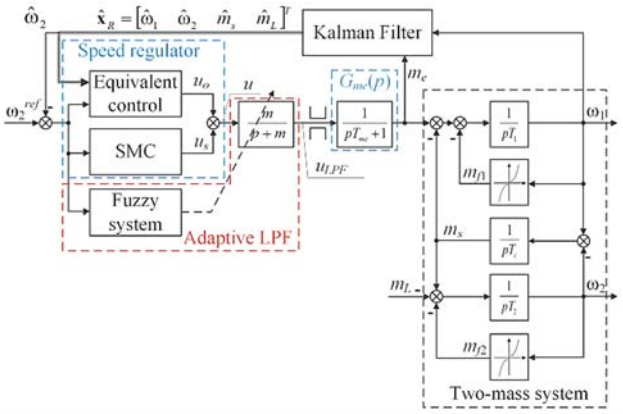


Fig. 1. Block diagram of the control structure

Figure 1 presents the control structure. There is the inner electromagnetic torque control loop, which is assumed to be a first degree inertia part with time constant $T_{me}$ (2).

$$G_{me}(p) = \frac{m_e}{m_e^{\text{ref}}} = \frac{1}{T_{me}p + 1} \tag{2}$$

where $p$ is the Laplace operator.

In the remaining part of this section, the speed controller is described. Sliding surface is chosen as below:

$$s = \mathbf{G}\mathbf{x} + \lambda \int_0^t e dt \tag{3}$$

where: $\mathbf{G} = [g_4, g_3, g_2, g_1]$ – gain vector, $\lambda$ – integrating gain, $e = \omega_2 - \omega_2^{\text{ref}}$ – regulation error, $s$ – sliding surface. The control law is a combination of two components

$$u = u_s + u_c \tag{4}$$

The component $u_c$ is a continuous one and it keeps the state vector on the reference trajectory. The component $u_s$ comes from the sliding-mode controller and is characterized by a high-frequency switching mode. It drives the system towards the sliding motion.

The components of the control law are described by Eqs. (5)–(7).

$$u_s = -\Gamma \operatorname{sgn}(s) \tag{5}$$

$$u_c = \mathbf{d}_1 \mathbf{x} + d_2 e + d_3 z \tag{6}$$

$$\begin{aligned} &\mathbf{d}_1 = -\left(\mathbf{GB}\right)^{-1} \mathbf{GA},\ d_2 = -\left(\mathbf{GB}\right)^{-1} \lambda, \\ &d_3 = -\left(\mathbf{GB}\right)^{-1} \mathbf{GD}_z,\ \mathbf{D}_z = \left[-1/T_2 \quad 0 \quad 0 \quad 0\right]^T \end{aligned} \tag{7}$$

where $z = \hat{m}_L$ – estimate of external disturbance, $\Gamma$ – controller gain, $\mathbf{d}_1$, $d_2$, $d_3$ – controller coefficients, $\mathbf{D}_z$ – simplified disturbance matrix

As shown in [8] and [17], a continuous controller can be tuned using the pole placement methods. Hence, while the described model is of fourth degree, the reference polynomial should have the same order (8).

$$p^4 \underbrace{1}_{b_4} + p^3 \underbrace{4\xi\omega_0}_{b_3} + p^2 \underbrace{\left(4\xi^2\omega_0^2 + 2\omega_0^2\right)}_{b_2} + p \underbrace{4\xi\omega_0^3}_{b_1} + \underbrace{\omega_0^4}_{b_0} = 0 \tag{8}$$

where: $\omega_0$ – given resonance pulsation, $\xi$ – given dumping coefficient, $b$ – coefficients of the reference polynomial. The tuning algorithm described above can be rewritten in the following form:

1. Calculate coefficients $b_4 - b_0$ of the reference polynomial (8) by choosing values of the coefficients $\omega_0$ and $\xi$.

2. Calculate the matrix $\mathbf{Q}_r$ using dependences for the matrix $\mathbf{M}$:

$$\mathbf{M} = \left[\mathbf{B} \quad \mathbf{AB} \quad \mathbf{A}^2\mathbf{B} \quad \mathbf{A}^3\mathbf{B}\right], \qquad \mathbf{M}^{-1} = \left[\mathbf{e}_1 \quad \mathbf{e}_2 \quad \mathbf{e}_3 \quad \mathbf{e}_4\right]^T \tag{9}$$

$$\mathbf{Q}_r = \left[ \mathbf{e}_4^T \quad \mathbf{e}_4^T\mathbf{A} \quad \mathbf{e}_4^T\mathbf{A}^2 \quad \mathbf{e}_4^T\mathbf{A}^3 \right]^T \tag{10}$$

3. Calculate the gain matrix **G**, gain + XB and the integration coefficient $\lambda$:

$$\mathbf{G} = \mathbf{g}\mathbf{Q}_r, \qquad g = \begin{bmatrix} b_1 & b_2 & b_3 & 1 \end{bmatrix}, \qquad \Gamma = \frac{b_0}{z(p)}, \qquad \lambda = \Gamma\left(\mathbf{GB}\right) \tag{11}$$

where: $z(p)$ is zero polynomial of the plant.

4. On the basis of the values obtained, calculate the other parameters: $\mathbf{d}_1$, $d_2$, $d_3$.

For details, a reader is referred to [8] and [17]. It can be easily checked whether the system is stable using the Lyapunov theory:

$$\begin{aligned} L &= s\dot{s} = s\left(\mathbf{G}\dot{\mathbf{x}} + \lambda e\right) = s\left(\mathbf{G}\left(\mathbf{A}x + \mathbf{B}u + \mathbf{D}_z z\right) + \lambda e\right) \\ &= s\left(\mathbf{GA}x + \mathbf{GB}\left[\mathbf{d}_1\mathbf{x} + d_2 e + d_3 z - \Gamma\,\mathrm{sgn}(s)\right] + \mathbf{GD}_z z + \lambda e\right) = -\Gamma\mathbf{GB}\left|s\right| \end{aligned} \tag{12}$$

Taking into account equation for $\lambda$ (11), the above equation takes the form

$$L = s\dot{s} = -\Gamma\mathbf{GB}\left|s\right| = -\lambda\left|s\right| < 0 \tag{13}$$

It results From Eq. (13), that system will be stable for $\lambda > 0$.

### 2.2. ADAPTIVE LOW PASS FILTER

Because of the unacceptable level of the chattering phenomenon in the original structure (ISMC), some modification was proposed to alleviate the chatter of the electromagnetic torque. The modification consists in applying the LPF to the output of the system. The filter could be described by the transfer function.

$$G_{LPF}(s) = \frac{u_{LPF}}{u} = \frac{m}{p+m} \tag{14}$$

where: $m$ denotes a bandwidth parameter of the filter, $u_{LPF}$ is the output value of the filter (proper control signal) and $u$ is its input value (unfiltered control signal).

It should be noted that the fixed bandwidth of the filter does not assure a good enough performance of the system due to the following reasons: for the wide bandwidth the dynamics are high but the chattering phenomenon is still big, on the other hand, for the narrow bandwidth the dynamics is low but the chattering phenomenon is eliminated. Thus, online adaptation of the bandwidth is proposed. The adaptation of the filter bandwidth is done by the Mamdani fuzzy-logic system. This system consists of three Gaussian and singleton membership functions (Fig. 2a).

The input value of the fuzzy-logic system is assumed to be the regulation error. The range of the input is limited to <–1, 1>. The output value of the fuzzy-logic system is

higher for the cases of high error values (the bandwidth is wide during dynamic states) and lower for the opposite cases (the bandwidth is narrow during static states).

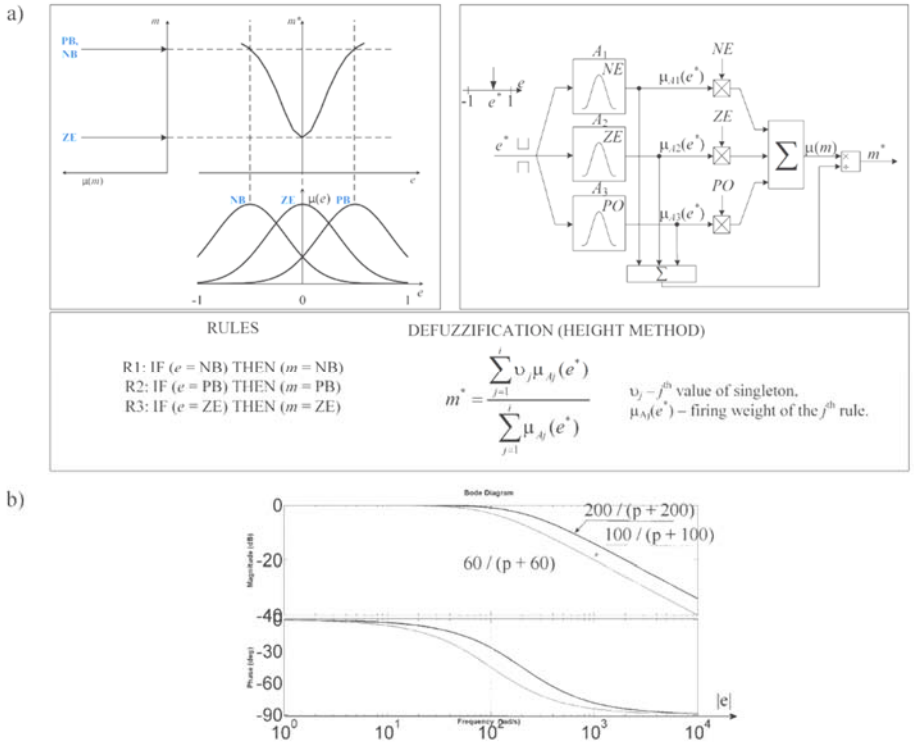


Fig. 2. Parameters of the fuzzy-logic block used to tune the bandwidth of the output LPF (a) and characteristics of the LPF for various values of the output of the fuzzy-logic system ($m^*$) (b)

The presented approach allows to mitigate the transients of the electromagnetic and the shaft torques and maintain high dynamics of the system simultaneously. The operating of the fuzzy-logic system is depicted in Fig. 2b.

### 2.3. KALMAN FILTER

The proposed control structure needs to have information about state variables of the plant. In order to keep track of the state variables the Kalman filter was implemented. The reason for it is the fact that the Kalman filter has good performance while operating in disturbed conditions.

In general, the system could be described as follows:

$$\dot{\mathbf{x}}_R = \mathbf{A}_R\mathbf{x}_R + \mathbf{B}_R\mathbf{u}_R + \mathbf{w}, \quad \mathbf{y}_R = \mathbf{C}_R\mathbf{x}_R + \mathbf{v} \tag{15}$$

where $\mathbf{x}_R$, $\mathbf{y}_R$ are the input and the output vectors, $\mathbf{A}_R$, $\mathbf{B}_R$, $\mathbf{C}_R$ are the state, input and output matrices of the system and $\mathbf{w}$, respectively, $\mathbf{v}$ represent process and measurement noises. After discretization of (15) with $T_s$ sampling step, the state estimation algorithm is calculated by [18]:

$$\hat{\mathbf{x}}_R(k+1/k+1) = \hat{\mathbf{x}}_R(k+1/k) + \mathbf{K}(k+1)\left[\mathbf{y}_R(k+1) - \mathbf{C}_R(k+1)\hat{\mathbf{x}}_R(k+1/k)\right] \quad (16)$$

where the gain matrix $\mathbf{K}$ is obtained according to the following numerical procedure:

$$\mathbf{P}(k+1/k) = \mathbf{A}_R(k)\mathbf{P}(k/k)\mathbf{A}_R(k)^T + \mathbf{Q}(k)$$

$$\mathbf{K}(k+1) = \mathbf{P}(k+1/k)\mathbf{C}_R(k+1)^T\left[\mathbf{C}_R(k+1)\mathbf{P}(k+1/k)\mathbf{C}_R(k+1)^T + \mathbf{R}\right]^{-1}$$

$$\mathbf{P}(k+1/k+1) = \left[\mathbf{I} - \mathbf{K}(k+1)\mathbf{C}_R(k+1)\right]\mathbf{P}(k+1/k)$$

where $\mathbf{P}$ is an estimate covariance, $\mathbf{I}$ is an identity matrix, $\mathbf{Q}$ and $\mathbf{R}$ are covariance matrices. The matrices of state, input and output, and the vector of state are defined as follows:

$$\mathbf{A}_R = \begin{bmatrix} 0 & 0 & -1/T_1 & 0 \\ 0 & 0 & 1/T_2 & -1/T_2 \\ 1/T_c & -1/T_c & 0 & 0 \\ 0 & 0 & 0 & 0 \end{bmatrix},\ \mathbf{B}_R = \begin{bmatrix} 1/T_1 & 0 & 0 & 0 \end{bmatrix}^T$$

$$\mathbf{C}_R = \begin{bmatrix} 1 & 0 & 0 & 0 \end{bmatrix},\ \hat{\mathbf{x}}_R = \begin{bmatrix} \hat{\omega}_1 & \hat{\omega}_2 & \hat{m}_s & \hat{m}_L \end{bmatrix}^T \quad (17)$$

The electromagnetic torque and the angular speed of the motor were chosen as input values:

$$\mathbf{u}_R = m_e, \qquad \mathbf{y}_R = \omega_1 \quad (18)$$

The matrices $\mathbf{Q}$ and $\mathbf{R}$ of the Kalman filter were tuned according to the Pattern Search procedure with the following cost function:

$$J = \int \Bigg( \left|\omega_1 - \hat{\omega}_1\right| \frac{d}{dt}\left|\omega_1 - \hat{\omega}_1\right| \left|\omega_2 - \hat{\omega}_2\right| \frac{d}{dt}\left|\omega_2 - \hat{\omega}_2\right| \left|m_s - \hat{m}_s\right| \frac{d}{dt}\left|m_s - \hat{m}_s\right| \frac{d}{dt}\left|m_L - \hat{m}_L\right| \frac{d}{dt}\left|m_L - \hat{m}_L\right| \Bigg) dt \quad (19)$$

The cost function defined as above guarantees good dynamics of estimation and minimization of noises in the estimated signals.

## 3. RESULTS OF THE SIMULATION TESTS

The presented model is described by the following time constants: $T_1 = T_2 = 203$ ms, $T_c = 1.2$ ms. The sampling step is $T_s = 500$ μs. As mentioned before, the transfer function of the torque control loop is assumed to be the first order one (2) and its time constant is $T_{me} = 2$ ms. The speed regulator was tuned using the presented algorithm for the parameters $\omega_0 = 45$ s$^{-1}$, $\xi = 0.7$ and the following parameters were obtained: $\Gamma = 1.0139$, $\lambda = 20\,503$.

During the simulation tests, the structure without a filter was investigated first. Thereafter, the filter of a constant bandwidth was introduced at the output of the speed regulator. It was shown that change of the bandwidth affects the chattering level of the electromagnetic torque, the dynamics of the system and the torsional vibrations. Finally, the structure with adaptive filter was examined.

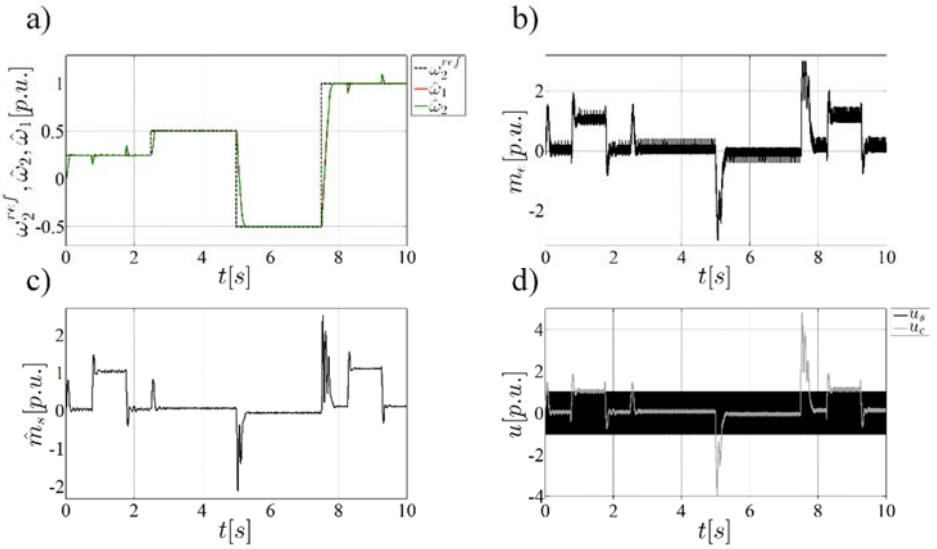


Fig. 3. Transients of angular velocities of the load (a), electromagnetic torque (b), shaft torque (c), and control signal (d); structure without any filter, results of simulation

Figure 3 depicts results of simulation obtained from the structure without a filter. It can be easily noticed that the electromagnetic torque oscillates very strongly (the chattering level is very high). It strongly affects the torsional vibrations.

The influence of the LPF on softening the chattering level is depicted in Figs. 4 and 5. It can be easily noticed that the lower the $m$, the lower the chattering level is but also the dynamics are somewhat lower. More importantly, for low $m$, the transient of angular velocity is distorted. In general, the use of the constant parameter filter decreases the torsional vibrations.

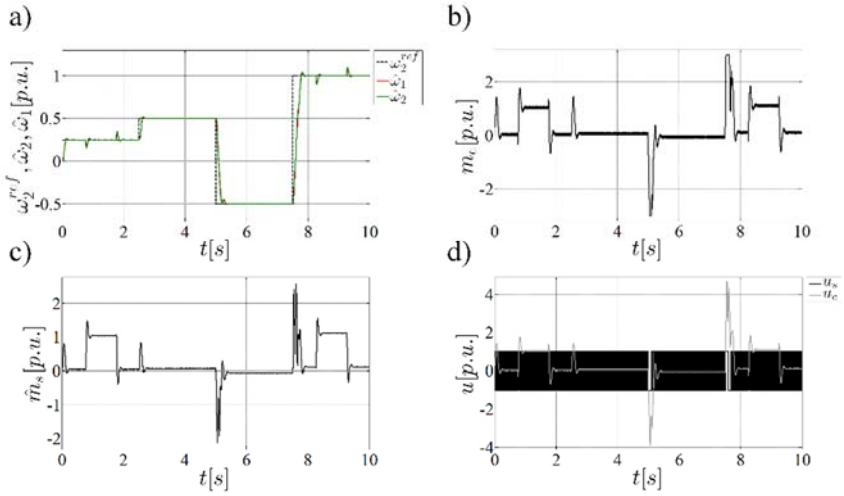


g. 4. Transients of angular velocities of the load (a), electromagnetic torque (b), shaft torque (c), and control signal (d); structure with the filter of constant bandwidth parameter $m = 45$, results of simulation

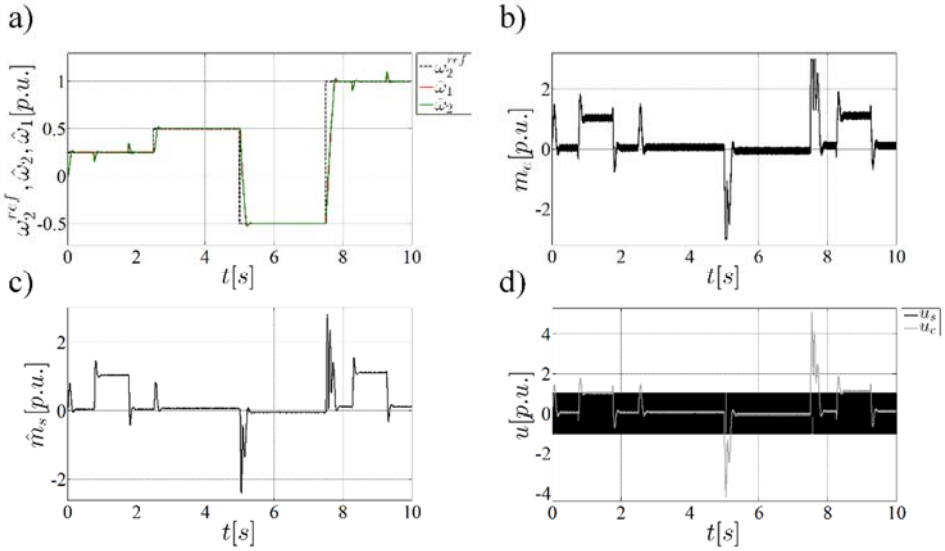


Fig. 5. Transients of angular velocities of the load (a), electromagnetic torque (b), shaft torque (c), and control signal (d); structure with the filter of constant bandwidth parameter $m = 140$, results of simulation

Thus, the adaptive low pass filter was proposed and implemented. The adaptation is realized by means of the fuzzy system (Fig. 2a). The parameters of the fuzzy system were chosen experimentally and they are as follows: the Gaussian membership functions $\sigma = 0.34$; $\mu = \{–0,5; 0; 0,5\}$, and the singletons: $ZE = –25$, $NB = PB = 150$.

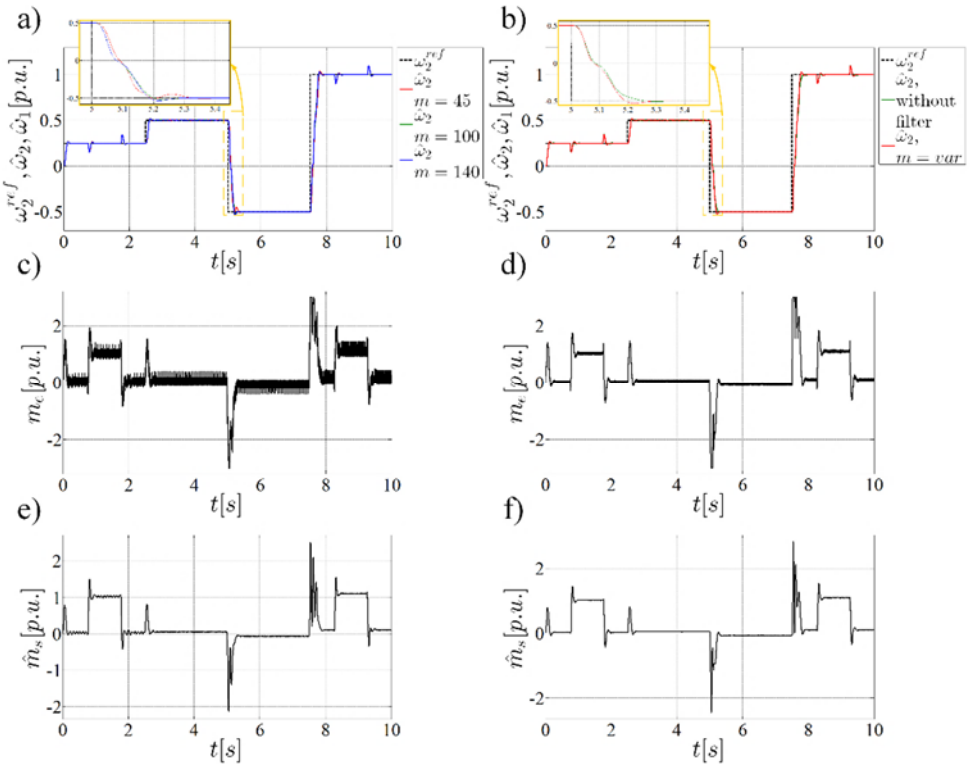


Fig. 6. Transients of angular velocities of the load (a, b), electromagnetic torque (c, d), and shaft torque (e, f); the filter bandwidth influence on the structure (a), comparison between structures with and without the adaptive filter (b), transients of the structure without filter (c, e), and with the adaptive filter (d, f); results of simulation

A comparison among transients of angular velocities is depicted in Fig. 6. The regulation of the bandwidth is crucial to preserve the dynamics of the system and the low chattering level without distortion of the velocity transient. It can be noticed that the adaptation works properly – dynamics of the system are retained as well as the chattering and the torsional vibrations are significantly lowered.

## 4. RESULTS OF THE EXPERIMENTAL TESTS

The experiment was conducted using two 500 W DC motors connected by a long, elastic shaft. The structure was controlled by a dSpace 1103 card. The experimental set is shown in Fig. 7.

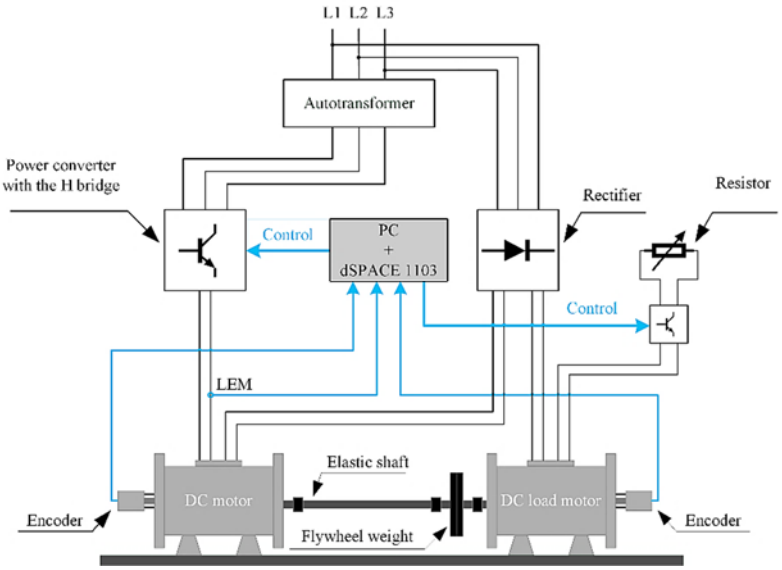


Fig. 7. Experimental set-up

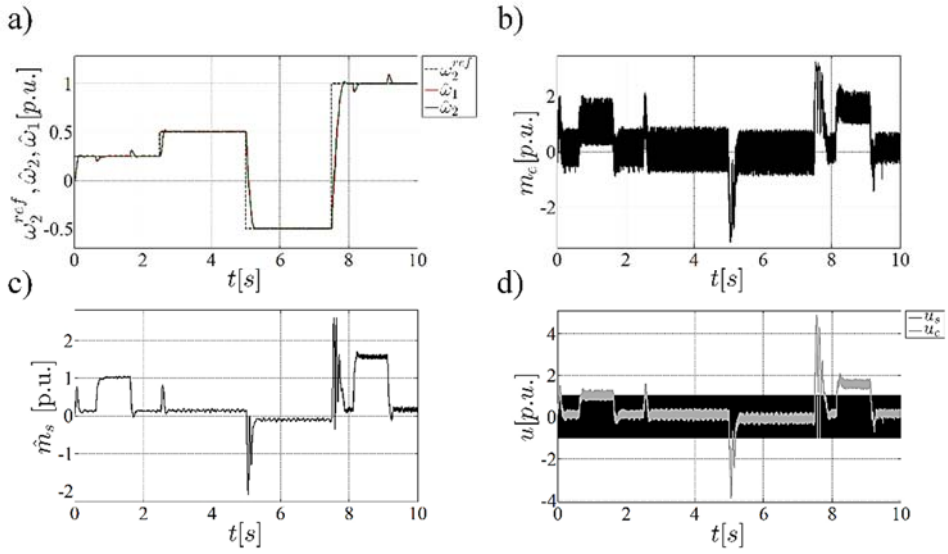


Fig. 8. Transients of angular velocities of the load (a), electromagnetic torque (b), shaft torque (c), and control signal (d); structure without filter, results of simulation

At the beginning, similarly as in case of simulation researches, the speed regulator was tuned according to the presented algorithm. The chosen parameters were the same as before, i.e. $\omega_0 = 45\ s^{-1}$, $\xi = 0.7$. The structure without a filter was examined first. The

results are shown in Fig. 8. As can be noticed based on the given transients, the system has assumed dynamic. Even though the character of the signals is similar to that obtained from simulations, the chattering effect is much greater.

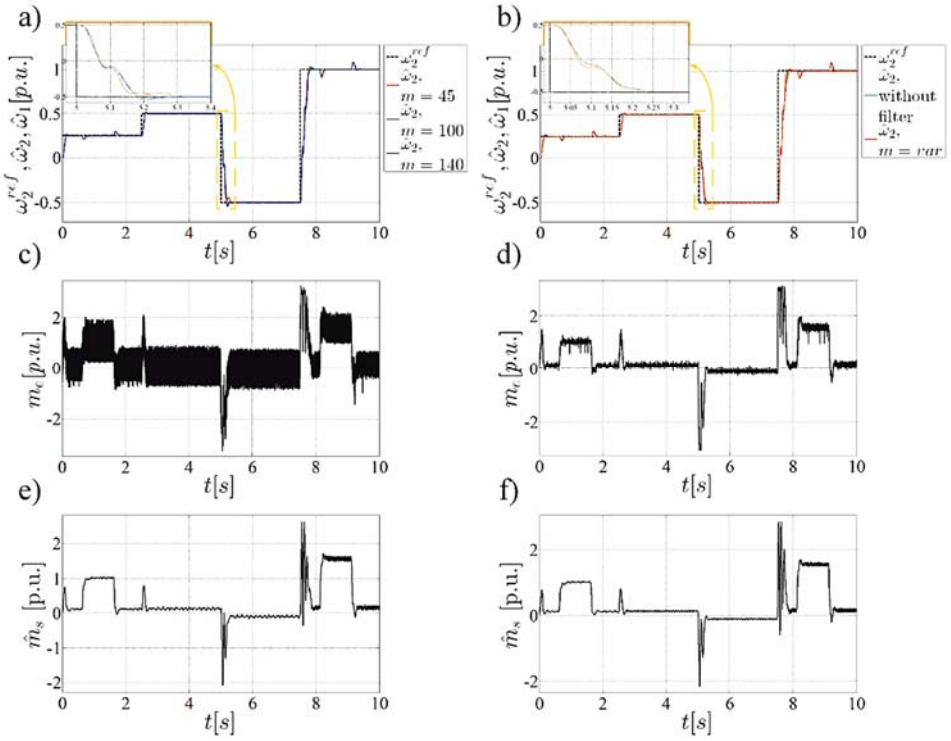


Fig. 9. Transients of angular velocities of the load (a, b), electromagnetic torque (c, d), and shaft torque (e, f); the filter bandwidth influence on the structure (a), comparison between structures with and without the adaptive filter (b), transients of the structure without the filter (c, e), and with the adaptive filter (d, f); results of simulation

Figure 9a presents the influence of the bandwidth of the filter on the characteristics of the bandwidth of the filter on the characteristics of the load and motor speeds. It can be easily noticed that the bandwidth with parameter $m = 100$ has good dynamics and rather small overshoot, while the ones with the bandwidth with parameters $m = 45$ and $m = 140$ have distorted transients and bigger overshoots. Thus, the regulation of the bandwidth is proposed to retain the dynamics and performance of the system without filter.

The structures without a filter and with the adaptive LPF (Fig. 9) react practically the same for the load appearing and start-up but a bit different for the return – there is a small overshoot in the structure with the adaptive filter. Most importantly, it can be noticed that chattering effect and the torsional vibrations are significantly lowered (Figs. 9c–f).

Finally, the same conclusion could be reached according to the experimental outcomes – the use of the output adaptive low pass filter does not affect strongly the shape of transient of the angular velocity but it allows to decrease the oscillations of the electromagnetic and the torsional torques significantly.

## 5. CONCLUSION

In this paper, the filtered integral sliding mode control (FISMC) for the electrical drive system with a flexible coupling was investigated. To calculate the control system parameters, the pole-placement method was implemented. The proposed structure relies on the adaptive low pass filter which allows to significantly soften the chattering effect and the torsional vibrations.

The influence of the bandwidth of the filter on the system performance was tested elaborately. On basis on the outcomes same concluding remarks can be formulated:

- The investigated control structures are working correctly. The design procedure is clear and relatively simple. The drawback of the classical algorithm is the chattering effect, which disturbs the characteristics of the system.
- In order to eliminate the chattering effect, the output low-pass filter is proposed. However, the selection of the bandwidths of the filter is a compromise between the chattering level and dynamic characteristics of the plant. During the static states, the bandwidth of the filter should be as low as possible. It guarantees the lowest chattering and suppression of torsional vibrations. During the dynamic states, the bandwidth should be greater to retain good dynamics of the system.
- The use of the adaptive low pass filter allows one to improve the performance of the integral sliding mode control (ISMC). It does not influence the dynamics of the system significantly, only somewhat bigger overshoots can appear during returns.
- The application of the fuzzy logic allows one to design the non-linear function of the changes of the bandwidth in relatively simple and intuitive way.
- The proposed control structures are examined under experimental tests. It proves that the proposed solutions are robust to un-modeled dynamics of the plant and measurements noises.

## REFERENCES

[1] FU J., WANG L., DU Y., ZHANG J., *A robust sliding mode control for nonlinear system with adjustable chattering phenomenon*, Variable Structures Systems (VSS), 14th International Workshop, IEEE, 2016, 34–38.

[2] BARTOSZEWICZ A., Non-switching reaching law for sliding mode control of discrete time systems, System Theory, Control and Computing (ICSTCC), 17th International Conference, IEEE, 2013, 60–65.

[3] LEI Q., WEIDONG Z., *Double-loop chattering-free adaptive integral sliding mode control for underwater vehicles*, OCEANS 2016, IEEE, Shanghai 2016, 1–6.
[4] SHEN C., SHENG Y., ZENG X., LIU X., *An improved chattering-free sliding mode control with finite time convergence for reentry vehicle*, Guidance, Navigation and Control Conference (CGNCC), IEEE Chinese, 2016, 69–74.
[5] HAI W., ZHIHONG M., HUIFANG K., YONG Z., MING Y., ZHENWEJ C., JINCHUAN Z., MANH T., *Design and implementation of adaptive terminal sliding-mode control on steer-by-wire equipped road vehicle*, IEEE Trans. Ind. Electr., 2016, 63 (9), 5774–5785.
[6] FENGJIAO G., XUEMEI R., *Extended state observer based adaptive integral sliding mode control for two inertia system*, Intelligent Human-Machine Systems and Cybernetics (IHMSC), 7th International Conference, IEEE, 2015, 483–486.
[7] TORCHANI B., SELLAMI A., GARCIA G., *Saturated sliding mode control for variable speed wind turbine*, The 5th International Renewable Energy Congress (IREC), Hammamet, Tunisia, 2014.
[8] ORŁOWSKA-KOWALSKA T., KAMIŃSKI M., SZABAT K., *Implementation of a sliding-mode controller with an integral function and fuzzy gain value for the electrical drive with an elastic joint*, IEEE Trans. Ind. Electr., 2010, 57(4), 1309–1317.
[9] BROCK S., *Hybrid P-PI sliding mode position and speed controller for variable inertia drive*, Przegl. Elektrotechn., 2014, 90(5), 29–34.
[10] JINKUN L., XINHUA W., *Advanced Sliding Mode Control for Mechanical Systems*, Springer, Tsinghua University Press, 2012.
[11] DRÓŻDŻ K., *Adaptive control of the drive system with elastic coupling using fuzzy Kalman filter with dynamic adaptation of selected coefficients*, Maint. Rel., 2015, 17(4), 561–568.
[12] FLUGGE-LOTZ I., *Discontinuous Automatic Control*, Princeton University Press, Princeton, New Jersey, 1953.
[13] ITKIS U., *Control Systems of Variable Structure*, Halsted Press, 1976.
[14] POORINEZHAD S., RAKHTALA S.M., *Chattering analysis of second order sliding mode algorithms for linear plants with disturbance*, Knowledge-Based Engineering and Innovation (KBEI), 2nd International Conference, IEEE, 2015, 101–105.
[15] SERKIES P., *Comparison of the control methods of electrical drives with an elastic coupling allowing to limit torsional torque amplitude*, Maint. Rel., 2017, 19(2), 203–210.
[16] SZABAT K., ORLOWSKA-KOWALSKA T., *Vibration suppression in a two-mass drive system using PI speed controller and additional feedbacks. Comparative study*, IEEE Trans. Ind. Electr., 2007, 54(2), 1193–1206.
[17] HUANG Y.J., WAY H.K., *Placing all closed loop poles of missile attitude control systems in the sliding mode via the root locus technique*, ISA Trans., 2001, 40(4), 333–340.
[18] SERKIES P., SZABAT K., *Estimation of the state variables of the two-mass system using fuzzy Kalman filter*, Ind. Electr. (ISIE), 2013 IEEE International Symposium, 2013, 1–6.